멀티홉 셀룰러 네트워크에서 릴레이 위치에 따른 하향링크 SINR 분석

정회원 조 성 현*, 문 성 호**

Downlink SINR Analysis of Multihop Cellular Networks according to Relay Positions

Sunghyun Cho*, Sungho Moon** *Regular Members*

요 약

본 논문은 멀티홉 셀룰러 네트워크에서 릴레이 노드의 배치 위치가 하향링크 SINR에 미치는 영향을 분석한다. 분석 모델에서는 릴레이 노드가 셀 안쪽으로 배치되는 것과 인접한 두 셀의 경계지역에 배치되는 두 가지 시나리오를 가정한다. 본 논문에서는 위 두 가지 시나리오의 하향링크 SINR을 비교 분석하기 위한 수학적 모델을 도출한다. 제안하는 수학적 모델에서는 멀티-셀 구조 및 셀 간 간섭 등을 고려한다. 수학적 분석 결과는 릴레이 노드들을 셀 안쪽에 배치하는 경우에 셀 간 간섭의 증가에도 불구하고 수신 신호 세기의 증가로 인해 릴레이 노드들을 셀 경계에 배치하는 경우에 비해 SINR이 증가함을 보인다.

Key Words : Multihop Cellular Networks, relay, Relay Positions, SINR, Interference

ABSTRACT

This paper studies the effect of the deployment position of the relay stations on the downlink signal-to-interference-noise-ratio (SINR) in multihop cellular networks. Two different relay deployment scenarios are considered where relay stations are located either inside cells or on the boundary among adjacent cells. The fundamental contribution is to compare fairly the average SINR between two scenarios with the proposed relay modeling framework that includes multi-cell geometries and inter-cell interferences. The mathematical results show that the SINR increases when relay stations are located inside cells because of higher received signal power.

Ⅰ. Introduction

In multihop cellular networks, technologies sometimes called relay technologies are applied to the current cellular networks to increase high-data-rate regions or to compensate for shadowing effect, which is mainly caused by large obstacles between transceivers[1,2]. Recently, the capacity of multihop cellular networks has been studied from the various points of view[3-5]. The performance of time-division multihop cellular networks, where a base station (BS) and relay stations (RSs) are multiplexed in the time domain, has been investigated in [3]. Reference [4] gives

※ 이 논문은 2008년도 정부재원(교육인적자원부 학술연구조성사업비)으로 한국학술진흥재단의 지원을 받아 연구되었음 (KRF-2008-331-D00331).

* 국립경상대학교 컴퓨터과학부 (dr.shcho@gnu.ac.kr), ** LG전자 이동통신연구소 (msungho@gmail.com)

논문번호 : KICS2010-04-145, 접수일자 : 2010년 4월 1일, 최종논문접수일자 : 2010년 5월 25일

upper bounds for multihop cellular networks with uniform placement of relays within a cell and evaluates the capacity from relays according to the number of hops. Reference [5] presents a relay-station-placement algorithm in high speed downlink packet access (HSDPA). This algorithm is an attempt to determine an optimal number of relay stations for a given data-rate threshold and determine appropriate locations of relay stations. The previous works well define the capacity of multihop cellular networks compared with single-hop networks. However, a SINR or capacity model of multihop cellular networks according to the position of relay stations has not been clearly defined, even though the placement of relay stations highly affects the SINR and capacity of multihop cellular networks. Therefore, this paper defines the typical relay station deployment scenarios and compares downlink SINR values between them by mathematical models.

Ⅱ. System Model

Figures 1(a) and 1(b) illustrate the considering relay deployment *Scenario 1* and *Scenario 2*, respectively. RSs are supposed to be located on the boundary among adjacent cells and controlled by the adjacent BSs as in *Scenario 1* that is better at reducing the total deployment number of RSs. Meanwhile, RSs are located inside cells and controlled by a base station (BS), as in *Scenario 2*. Many previous works[3,4] assume that RSs are located inside cells and controlled by a base station (BS), as in *Scenario 2*, because it is favorable to increase cell radiuses or high-data-rate regions. The frequency-reuse factor (FRF) of both scenarios is assumed to be one, which means that all BSs and RSs share the same spectrum band. Therefore, the resources of a BS and RSs should be coordinated for multiplexing. This paper mainly considers time division multiplexing (TDM) between a BS and RSs. It is assumed that the transparent-mode frame structure defined in IEEE 802.16j[6] is used in the proposed mathematical models. The timing of every frame is assumed to be synchronized between

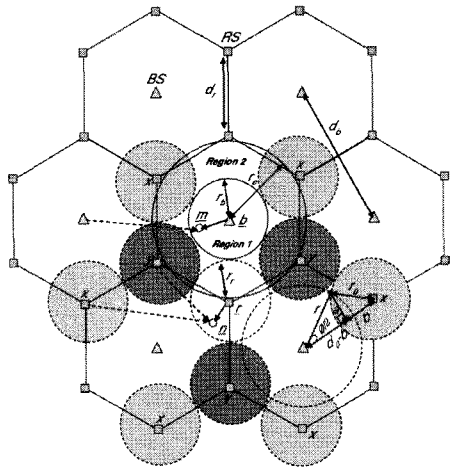

(a) Relay deployment scenario 1

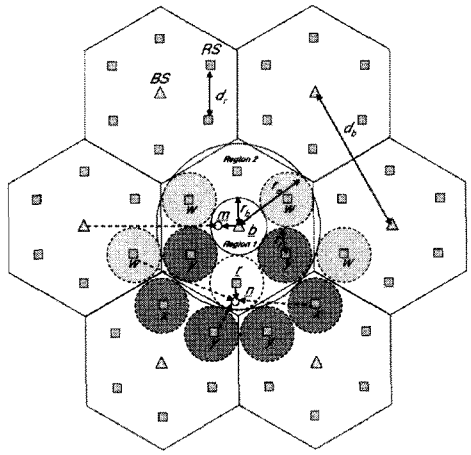

(b) Relay deployment scenario 2

Fig. 1. Relay deployment scenarios

adjacent BSs and the duplexing between downlink and uplink is based on time division duplexing.

Ⅲ. The SINR Analysis

This section proposes an analysis of the received SINR values from mathematical models for *Scenarios 1* and *2*. The model assumes that a perfect equalization and an OFDM transmission completely compensate for fast fading and intra-cell interferences, respectively. Large-scale fadings such as propagation loss and shadow fading are considered with uniformly distributed mobile stations (MSs) in seven cells.

3.1 Relay Deployment Scenario 1

As shown in Fig.1(a), two regions are defined in each cell. The first region defined by an equivalent radius of r_b is a circled area where MSs are served by a BS. The second one is a doughnut-shaped region which is defined by two radiuses, r_b and r_e. In the second region, all MSs have communications with relay stations. In Region 1, the received signal power at an MS $\underline{m}$ from a BS $\underline{b}$, $P^{(r)}_{\underline{b}\to\underline{m}}$ is calculated as:

$$P^{(r)}_{\underline{b}\to\underline{m}} = \alpha_{\underline{m}} P^{(t)}_{BS} \cdot r^{-\gamma}_{\underline{b}\to\underline{m}} \cdot 10^{-\zeta_{\underline{b}\to\underline{m}}/10}, \quad (1)$$

where $P^{(t)}_{BS}$, $\alpha_{\underline{m}}$, γ, and $\zeta_{\underline{b}\to\underline{m}}$ denote the maximum transmission power of a BS, the proportion of the allocated resources for the MS $\underline{m}$ to the whole downlink resources, an attenuation constant, and a log-normal shadow fading, respectively.

The received interference power at MS $\underline{m}$, $I^{(r)}_{\underline{m}}$ is derived as [7]:

$$I^{(r)}_{\underline{m}} = \frac{\theta_b}{360^\circ} \sum_{z \neq \underline{b}} \left\{ \sum_{j \in z} \left(\alpha_j P^{(t)}_{BS} \right) \cdot r^{-\gamma}_{z\to\underline{m}} \cdot 10^{-\zeta_{z\to\underline{m}}/10} \right\}, \quad (2)$$

where θ_b, z, and j represent a main lobe width of sectored cells, an index of adjacent BSs around BS $\underline{b}$, and an index of MSs, respectively. From Eqs. (1) and (2), the received SINR for MS $\underline{m}$ in Region 1 can be defined as $E[P^{(r)}_{\underline{b}\to\underline{m}} / (I^{(r)}_{\underline{m}} + N_0)]$. Since $P^{(r)}_{\underline{b}\to\underline{m}}$ and $I^{(r)}_{\underline{m}}$ are i.i.d in the proposed model, the lower bound of the received SINR for MS $\underline{m}$ in Region 1 can be derived by Jensen's inequality as follows:

$$\begin{aligned} \Gamma^{(r)}_{\underline{b}\to\underline{m}} &= \frac{E\left[P^{(r)}_{\underline{b}\to\underline{m}}\right]}{E\left[I^{(r)}_{\underline{m}}\right] + N_0} \\ &\simeq \frac{\overline{\alpha_b} P^{(t)}_{BS} \cdot \mathrm{F}_{-\gamma}(r_b, \epsilon_b) \cdot \mathrm{S}(\zeta_{\underline{b}\to\underline{m}})}{\frac{\theta_b}{360^\circ} \sum_{z \neq \underline{b}} \left(\overline{\alpha_b} P^{(t)}_{BS} \cdot \overline{\delta_b} \cdot \mathrm{G}_{-\gamma}(r_b, d_b) \cdot \mathrm{S}(\zeta_{z\to\underline{m}}) \right) + \mathrm{N}_0} \\ &\simeq \frac{\overline{\alpha_r} P^{(t)}_{BS} \cdot \mathrm{F}_{-\gamma}(r_b, \epsilon_b) \cdot \mathrm{S}(\zeta_{\underline{b}\to\underline{m}})}{\frac{\overline{\alpha_b} P^{(t)}_{BS} \cdot \theta_b \cdot 6}{360^\circ} \cdot \frac{\overline{\delta} r_b^2}{r_e^2} \cdot \mathrm{G}_{-\gamma}(r_b, d_b) \cdot \mathrm{S}(\zeta_{z\to\underline{m}}) + \mathrm{N}_0} \end{aligned} \quad (3)$$

where $\overline{\alpha_b}$, $\overline{\delta_b}$, and $\overline{\delta}$ denote the mean resource allocation ratio, the average number of active MSs within a radius of r_b, and the average number of active MSs in an entire cell, respectively. Moreover, functions $\mathrm{F}_n(r,d)$ and $\mathrm{G}_n(r,\epsilon)$ represent the expectations of propagation loss terms, and $\mathrm{S}(\zeta)$ is the expectation of shadow fading ζ. The detailed derivations of these functions are presented in Appendix.

In Region 2, an MS $\underline{n}$ is served by RS $\underline{r}$, and is interfered by the three nearest neighbor RSs indexed by y and the six second nearest neighbor RSs indexed by x, which are located at a distance of $\sqrt{3}\,d_r$ from RS $\underline{r}$. The radius of RS cell, r_r is equal to $(r_e - r_b)$ in this scenario. Thus, the lower bound of the received SINR of MS $\underline{n}$ can be expressed as:

$$\begin{aligned} \Gamma^{(r)}_{\underline{r}\to\underline{n}} &= \frac{E\left[P^{(r)}_{\underline{r}\to\underline{n}}\right]}{E\left[I^{(r)}_{\underline{n}}\right] + N_0} \\ &\simeq \overline{\alpha_r} P^{(t)}_{RS} \cdot \mathrm{F}_{-\gamma}(r_r, \epsilon_r) \cdot \mathrm{S}(\zeta_{\underline{r}\to\underline{n}}) \\ &\quad \Big/ \left\{ \frac{\overline{\alpha_r} P^{(t)}_{RS} \cdot \theta_r}{360^\circ} \cdot \frac{\overline{\delta} r_r^2}{r_e^2} \cdot (3\mathrm{G}_{-\gamma}(r_r, d_r) \cdot \mathrm{S}(\zeta_{y\to\underline{n}}) \right. \\ &\quad \left. + 6\mathrm{G}_{-\gamma}(r_r, \sqrt{3}\,d_r) \cdot \mathrm{S}(\zeta_{x\to\underline{n}})) + N_0 \right\}, \end{aligned} \quad (4)$$

where $P^{(t)}_{RS}$, $\overline{\alpha_r}$, and θ_r denote the maximum transmission power of a RS, the mean resource allocation raio of an MS served by a RS, and a main lobe width of sectored RSs, respectively.

3.2 Relay Deployment Scenario 2

Like *Scenario 1*, two regions are defined as shown in Fig. 1(b). In Region 1, all derivations are the same as the relay deployment *Scenario 1* because the equivalent radius of Region 1 is also set to r_b. Thus, the lower bound of the received SINR for MS $\underline{m}$ in Region 1 is the same as Eq. (3).

In Region 2, there are three types of major interferers for a given MS $\underline{n}$ served by RS $\underline{r}$. The most significant interferers are the four nearest RSs indexed by y. The second group of interferers indexed by x are two neighbor RSs at a distance of $\sqrt{2}\,d_r$ from RS r. There exist the four third nearest neighbor RSs indexed by w at a distance of $\sqrt{3}\,d_r$.

The other RSs located farther can be ignored like relay deployment *Scenario 1*. Therefore, the lower bound of the received SINR for MS $\underline{n}$ in Region 2 can be derived as:

$$\Gamma^{(r)}_{\underline{r}\to\underline{n}} = \frac{E\left[P^{(r)}_{\underline{r}\to\underline{n}}\right]}{E\left[I^{(r)}_{\underline{n}}\right]+N_0} \simeq \overline{\alpha_r} P^{(t)}_{RS} \bullet \mathrm{F}_{-\gamma}(r_r,\epsilon_r) \bullet \mathrm{S}(\zeta_{\underline{r}\to\underline{n}}) \Bigg/ \left\{ \begin{array}{l} \dfrac{\overline{\alpha_r} P^{(t)}_{RS} \bullet \theta_r}{360^\circ} \bullet \dfrac{\overline{\delta} r_r^2}{r_e^2} \bullet (4\mathrm{G}_{-\gamma}(r_r,d_r) \bullet \mathrm{S}(\zeta_{y\to\underline{n}}) \\ +2\mathrm{G}_{-\gamma}(r_r,\sqrt{2}\,d_r) \bullet \mathrm{S}(\zeta_{x\to\underline{n}}) \\ +4\mathrm{G}_{-\gamma}(r_r,\sqrt{3}\,d_r) \bullet \mathrm{S}(\zeta_{w\to\underline{n}})) + N_0 \end{array} \right\}, \quad (5)$$

where r_r and d_r are $(r_e\text{-}r_b)/2$ and (r_b+r_r), respectively, in this scenario.

3.3 Numerical example and discussion

For a fair comparison, the average SINR $\overline{\Gamma^{(r)}}$ can be defined as the weighted sum of SINR values for two regions, and can be expressed as:

$$\overline{\Gamma^{(r)}} = \frac{r_b^2}{r_e^2} \bullet I^{(r)}_{\underline{b}\to\underline{m}} + \left(1-\frac{r_b^2}{r_e^2}\right) \bullet I^{(r)}_{\underline{r}\to\underline{n}} \quad (6)$$

All shadow fadings are assumed to be identical to ζ_0. Table 1 shows the detailed parameter set for a numerical example. Fig. 2 shows the average SINR of *Scenarios 1*, *2*, and single-hop cellular network. The offered load becomes 100% when the number of MSs per cell is 100 because $\overline{\alpha_b}$and $\overline{\alpha_r}$ are set to 0.01. As the number of MSs per cell increases, the average SINR values decrease due to the increased interference. As shown in the result, the average SINR in multihop cellular network is larger than in single-hop cellular network. In addition, as it can be expected from Eqs. (4) and (5), the average SINR in *Scenario 2* is larger than in *Scenario 1* for every cases due to higher signal power strength in Region 2. Especially, the SINR difference between *Scenarios 1* and *2* increases as the relay-cell radius becomes larger.

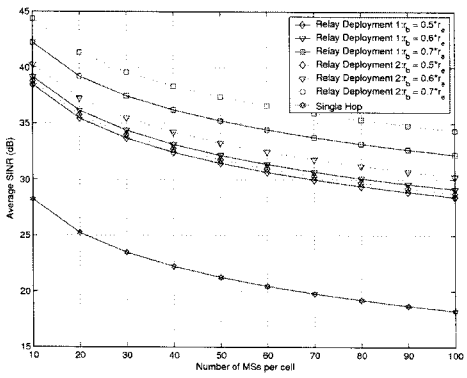

Fig. 2. Average downlink SINR

Table 1. Parameters for numerical example

Parameter	Value	Parameter	Value
$\overline{\alpha_b}$	0.01	$\overline{\alpha_r}$	0.01
$P_{max,BS}$	42 [dBm]	$P_{max,RS}$	30 [dBm]
θ_b	360°	θ_r	360°
ϵ_b	10 [m]	ϵ_r	10 [m]
r_e	1000 [m]	d_b	$\sqrt{3}\,r_e$
γ	4	N_o	-174 [dBm]
σ_{ζ_0}	8 [dB]		

Ⅳ. Conclusions

This paper proposes the average SINR models for two different relay deployment scenarios taking into consideration multi-cell geometries and inter-cell interferences. The proposed mathematical models prove that *Scenario 2* has better performance than *Scenario 1* in terms of SINR. However, there exist a clear trade-off between the SINR gain and the deployment cost because *Scenario 2* requires larger number of RSs per cell even though it has better SINR. In addition, if we consider the implementation overhead of relay systems such as resource sharing and signaling overhead between BSs and RSs, the system capacities may not exactly correspond to the SINR models. Therefore, it is for further study to extend this work to analyze the capacities of multihop cellular networks according to relay positions, and to find optimal relay deployment positions for maximizing the capacities with due regard to implementation overhead.

Appendix

1. Expectations of pathloss terms and shadow fading

With a given cell with a radius of r_0, we can define two types of random variables, which represent specific distances. First, a random variable R_1 represents a distance from the center of the cell to an MS located within a radius of r_0. If MSs are uniformly distributed in the cell, the minus γ-th moment of R_1 can be derived as:

$$\begin{aligned} &\mathrm{F}_{-\gamma}(\mathrm{r}_0,\epsilon_0) \\ &= \int_{\epsilon_0}^{r_0} r^{-\gamma} f_{R_1}(r)dr \\ &= \int_{\epsilon_0}^{r_0} \frac{2r^{-\gamma+1}}{r_0^2-\epsilon_0^2}dr = \frac{2\cdot(r_0^{-\gamma+2}-\epsilon_0^{-\gamma+2})}{(r_0^2-\epsilon_0^2)\cdot(-\gamma+2)}, \end{aligned} \tag{7}$$

where ϵ_0 denotes the minimum distance between a BS and an MS.

Second, we can define a random variable R_2 which represents a distance from a point outside of the given cell to an MS within the cell. The probability density function $f_{R_2}(r)$ can be approximated from Fig. 3, where a and b denote the length of a perpendicular line from the cross point to the base line and the distance from the center of the cell to a contact point between the perpendicular line and the base line, respectively. From trigonometrical functions, we can obtain the following equations:

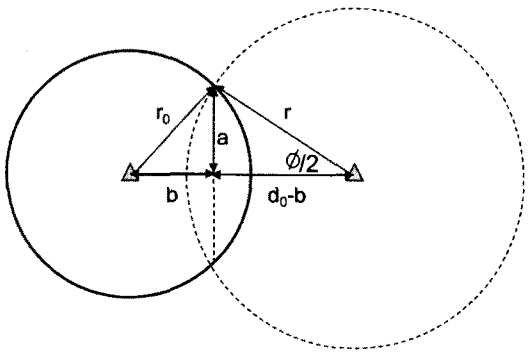

Fig. 3. Probability density function for R_2

$$a^2+b^2=r_0^2, \tag{8}$$

$$r\sin(\phi/2)=a, \tag{9}$$

$$r\cos(\phi/2)=d_0-b. \tag{10}$$

Using above three equations, we can obtain ϕ and thus, the minus γ-th moment of R_2 can be derived as:

$$\begin{aligned} &\mathrm{G}_{-\gamma}(\mathrm{r}_0,\mathrm{d}_0) \\ &= \int_{d_0-r_0}^{d_0+r_0} r^{-\gamma}\cdot f_{R_2}(r)dr \\ &= \int_{d_0-r_0}^{d_0+r_0} r^{-\gamma}\cdot\frac{r\phi}{\pi r_0^2}dr \\ &= \int_{d_0-r_0}^{d_0+r_0}\frac{2r^{-\gamma+1}}{\pi r_0^2}\cdot\cos^{-1}\left(\frac{r^2+d_0^2-r_0^2}{2rd_0}\right)dr, \end{aligned} \tag{11}$$

where d_0 denotes a distance from the center of the cell to a specific point outside of the cell.

Typically, shadowing in a wireless channel is modelled as a log-normal distribution with zero mean. Thus, the expectation of a log-normally distributed random variable with a mean of $m_\zeta=0$ and a variance of σ_ζ^2 is written as:

$$\begin{aligned} \mathrm{S} &= 10^{-m_\zeta/10}\cdot\exp\left\{\frac{\left(\frac{\ln 10}{10}\sigma_\zeta\right)^2}{2}\right\} \\ &= \exp\left\{\frac{\left(\frac{\ln 10}{10}\sigma_\zeta\right)^2}{2}\right\}. \end{aligned} \tag{12}$$

References

[1] R. Pabst et al., "Relay-based deployment concepts for wireless and mobile broadband radio," *IEEE Commun. Mag.*, Vol.42, No.9, pp.80-89, Sep. 2004.

[2] H. Wu, C. Qiao, S. De, and O. Tonguz, "Integrated cellular and Ad Hoc relaying systems: iCAR," *IEEE J. Select. Areas Commun.*, Vol.19, No.10, pp.2105-2115, Oct. 2001.

[3] N. Esseling, B. H. Walke, and R. Pabst,

"Performance evaluation of a fixed relay concept for next generation wireless systems," *in Proc. IEEE PIMRC 2004*, Vol.2, pp.744-751, Sep. 2004.

[4] S. Mukherjee and H. Viswanathan, "Analysis of throughput gains from relays in cellular networks," *in Proc. IEEE Globcom 2005*, Vol.6, pp.6, Dec. 2005.

[5] W. Hung-yu, S. Ganguly, and R. Izmailov, "Ad hoc relay network planning for improving cellular data coverage," *in Proc. IEEE PIMRC 2004*, Vol.2, pp.769-773, Sep. 2004.

[6] IEEE 802.16j Baseline Document for Draft Standard, "Part 16: Air interface for fixed and mobile broadband wireless access systems - multihop relay specification," Apr. 2007.

[7] S. H. Moon, S. Park, J. K. Kwon, and D. K. Sung, "Capacity improvement in CDMA downlink with orthogonal code-hopping multiplexing," *IEEE Trans. on Vehic. Tech.*, Vol.55, No.2, pp.510-527, Mar. 2006.

조 성 현 (Sunghyun Cho) 정회원

1995년 2월 한양대학교 컴퓨터 공학과 공학사
1997년 2월 한양대학교 컴퓨터 공학과 공학석사
2001년 8월 한양대학교 컴퓨터 공학과 공학박사
2009년 9월~현재 경상대학교 컴퓨터과학부 조교수
2006년 10월~2008년 2월 Stanford University, Postdoctoral Visiting Scholar
2001년 9월~2006년 10월 삼성종합기술원 및 삼성전자 정보통신연구소 전문연구원
<관심분야> 차세대 이동통신 시스템, 자동차 통신

문 성 호 (Sungho Moon) 정회원

1999년 2월 한국과학기술원 전자전산학과 공학사
2001년 2월 한국과학기술원 전자전산학과 공학석사
2006년 8월 한국과학기술원 전자전산학과 공학박사
2007년~현재 LG전자 이동통신연구소 책임연구원
2006년 9월~2007년 8월 Stanford University, Postdoctoral Visiting Scholar
<관심분야> IEEE 802.16m, 3GPP LTE-A Standard, 3G & 4G, 물리계층 기술